International Journal of Chemical, Materials and Biomolecular Sciences
ISSN: 2415-6620
Vol:14, No:9, 2020

Influence of Silica Surface Hydrophilicity on Adsorbed Water and Isopropanol Studied by in-situ NMR

Hyung T. Kwak, Jun Gao, Yao An, Alfred Kleinhammes, Yue Wu

***Abstract*—**Surface wettability is a crucial factor in oil recovery. In oil industry, the rock wettability involves the interplay between water, oil, and solid surface. Therefore, studying the interplay between adsorptions of water and hydrocarbon molecules on solid surface would be very informative for understanding rock wettability. Here we use the in-situ Nuclear Magnetic Resonance (NMR) gas isotherm technique to study competitive adsorptions of water and isopropanol, an intermediate step from hydrocarbons. This in-situ NMR technique obtains information on thermodynamic properties such as the isotherm, molecular dynamics via spin relaxation measurements, and adsorption kinetics such as how fast the system can reach thermal equilibrium after changes of vapor pressures. Using surfaces of silica glass beads, which can be modified from hydrophilic to hydrophobic, we obtained information on the influence of surface hydrophilicity on the state of surface water via obtained thermodynamic and dynamic properties.

***Keywords*—**Competitive adsorption, nuclear magnetic resonance, wettability.

I. Introduction

WETTABILITY is one of the most important parameters influencing the hydrocarbon reservoir behavior such as estimated ultimate recovery. It describes the preference of a solid to be in contact with one fluid versus another [1]. It is one of the most important parameters influencing the hydrocarbon reservoir behavior such as estimated ultimate recovery. One of the most standard ways to quantify wettability in oil industry is using the contact angle method, which measures the angle between the water-oil interface and the water-solid (or oil-solid) interface. However, in addition to microscopic surface properties, there are many other factors that could also influence the contact angle measurement such as surface rugosity. Moreover, direct contact angle measurement is impossible for rock pore surfaces. There are a few empirical methods for characterizing wettability, such as the Amott-Harvey (AH) method [2] and the United States Bureau of Mines (USBM) method [3], but their connections with contact angle are very obscure. Therefore, new methods for determining wettability for rock samples are highly desirable. NMR is one of the most useful techniques that can provide quantitative information noninvasively on fluid inside pore structures of rock samples. NMR has been used extensively on wettability study [4]-[9]. It is shown that T_1 and T_2 relaxation times of water inside pores of rock samples are sensitive to surface properties. ^{1}H NMR relaxation times of water near the surface are strongly altered and through rapid exchange the relaxation times of water confined inside pores are also influence. In this study, we use the in-situ NMR technique to measure the thermodynamic properties, namely the adsorption isotherms, for water and isopropanol (IPA), as well as the behavior of their competitive adsorption. This allows us to study in-situ adsorbed surface layers exclusively. This provides a sensitive technique to probe the influence of surface hydrophilicity on the thermodynamic state and the dynamics of adsorbed water.

Hyung T. Kwak* and Jun Gao are with the Saudi Aramco, Dhahran, Saudi Arabia, 31311 (*e-mail: hyung.kwak@aramco.com).

Yao An, Alfred Kleinhammes and Yue Wu are with the Department of Physics and Astronomy, University of North Carolina, Chapel Hill, NC 27599-3255, USA

II. Experimental Detail

A. Materials

9-13 μm glass spheres are purchased from Sigma-Aldrich and used without further purification. The ingredient of glass spheres is SiO_2. Sulfuric acid solution 4N from Fisher Scientific and chloro(dodecyl)dimethylsilane from Sigma-Aldrich are used for hydrophilic and hydrophobic treatment, respectively.

B. Surface Wettability Modification

For hydrophilic treatment, 4 g as-received 10 μm glass beads are loaded into the glass bottle with 55 mL of 4N sulfuric acid solution and held for 72 hours at 70 ± 10 °C. Glass bottle is immersed in the silicon oil bath for homogeneous heating. The treated sample is then washed with 1000 mL deionized water 3 times and each time for 24 hours to remove acid residues and then dried in desiccator for another 3 days. The hydrophobic treatment uses the silane-coating method. The length of the hydrophobic tail influences the hydrophobicity. [10] The mixing also takes 72 hours but under 40 °C. After that, ethanol is used to clean up all remaining organic materials.

C. In-situ NMR Detected Isotherm System

The water and IPA isotherms are measured by using a 380-MHz Oxford NMR instrument with home-made glass vacuum and vapor control system equipped with computer interfaced pressure gauge and mechanical pump. Fig. 1 shows the schematic diagram of this system. The pressure is acquired by using BARATHON from MKS and NI USB-6008 from National Instruments. The measurement temperature is 18.0 °C, corresponding to a saturated vapor pressure of 15.49 Torr

for water and 27.92 Torr for IPA. The chemical shift reference is TMS.

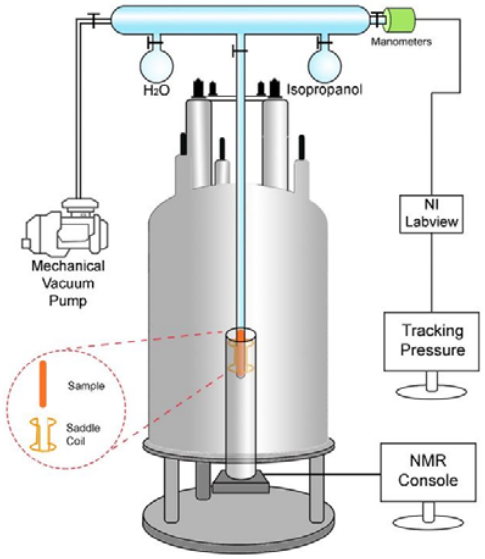

Fig. 1 Schematic diagram of *in-situ* NMR-detected isotherm system

III. Results and Discussions

Fig. 2 (a) shows the water adsorption isotherm on 10 µm untreated glass beads. In Fig. 2 (a), when the relative pressure (P/P_0) is below 0.5, the isotherm is rather linear. In this region, the adsorption is mainly governed by water interactions with the surface. In the inset of Fig. 2 (a), we show the estimated number of layers of adsorbed water. Equations (1)-(3) are used for this estimation. 0.37 nm is used for the diameter of water on surface. Less than 6 layers of water are adsorbed on the surface.

$$\frac{\frac{L_{coil}}{L_{sample-length}}\cdot m_{sample}}{\frac{\rho_{sample}}{V_{sample}}}\cdot S_{one-sphere} = S_{total-sphere} \quad (1)$$

$$S_{total-sphere}\cdot d_{water}\cdot \rho_{water} = m_{water} \quad (2)$$

$$d_{water} = d_{water-one-layer}\cdot n_{number-of-layers} \quad (3)$$

Increasing P/P_0 above 0.6, faster and nonlinear growth of adsorption versus P/P_0 occurs indicating stronger influence of water-water interactions and cooperativity. As shown in Figs. 2 (b) and (c), both spin-lattice relaxation time T_1 and spin-spin relaxation time T_2 undergo sharp jumps above P/P_0 = 0.6 demonstrating a qualitative change of the state of adsorbed water above P/P_0 = 0.6. The T_1/T_2 ratio is about 1200 below P/P_0 = 0.6. Such extremely large T_1/T_2 ratio indicates that the adsorbed water molecules have restricted mobility. The T_1/T_2 ratio decreases suddenly to less than 400 above P/P_0 = 0.6, indicating the growth of more bulk-like water above the surface water with restricted mobility. Within the relaxation measurement time scale, surface water with restricted mobility and the more bulk-like water undergo exchanges giving rise to single exponential decays in the T_1 and T_2 relaxation measurements. The growth of the bulk-like water could be initiated at the narrow gaps between particles.

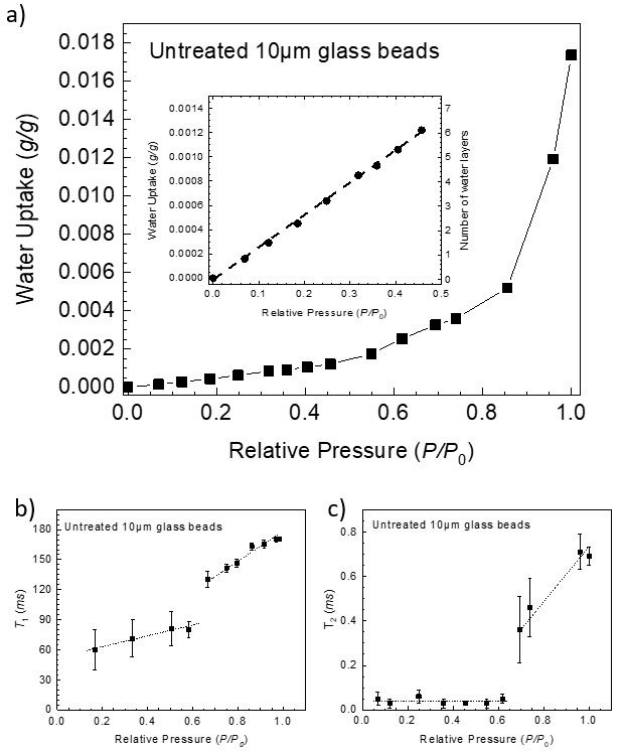

Fig. 2 (a) 10 µm untreated glass beads, water adsorption isotherm, (b) ^{1}H spin-lattice relaxation time at different loading levels, (c) ^{1}H spin-spin relaxation time at different loading levels

Fig. 3 shows the kinetic information of water adsorption and it also reveals the qualitative differences between adsorption below P/P_0 = 0.6 and adsorption above P/P_0 = 0.6. As shown in Fig. 3 (a), when the particles are exposed to water vapor below P/P_0 = 0.6, the adsorption reaches equilibrium with a time constant of 11 minutes, consistent with surface adsorption. In contrast, when changing the vapor pressure above P/P_0 = 0.6, such as from 0.736 to 0.815 as shown in Fig. 3 (b), the adsorption reaches equilibrium with a very large time constant of about 220 minutes. This much larger time constant indicates that the adsorption above P/P_0 = 0.6 is a nucleation process requiring very long time to reach a critical nucleation size at the narrow gaps between particles.

Fig. 4 (a) shows IPA adsorption isotherms on 10 µm untreated glass beads with different amount of pre-adsorbed water. The amount of IPA uptake in unit of g/g is comparable to water uptake shown in Fig. 2 (a) but is about 3 times lower in unit of mol/g. The influence of pre-adsorbed water on IPA adsorption is negligible until the pre-adsorbed water is at the level above $P_{water}/P_{0\text{-water}}$ = 0.5. Thus, the surface water with restricted mobility discussed earlier has negligible effect on IPA adsorption. Pre-adsorption of condensed water (P_{water}/

$P_{0\text{-water}} > 0.6$) does reduce IPA adsorption as IPA access to the solid surface is largely sealed by condensed water. IPA can still adsorb via different mechanism such as through mixing with condensed water. This argument can be verified by the influence of pre-adsorbed water on the -CH_3 proton spin-lattice relaxation T_1 of IPA. Fig. 4 (b) shows the -CH_3 proton T_1 of IPA (loaded at the level of $P_{IPA}/P_{0\text{-IPA}} = 0.83$), as a function of the level of pre-adsorbed water. The pre-adsorbed water has no effect on IPA T_1 until $P_{water}/P_{0\text{-water}} > 0.5$. Thus, surface water with restricted mobility does not have any effect on IPA T_1, consistent with its negligible effect on IPA adsorption isotherm. Both the isotherms and T_1 data indicate that surface adsorbed water with restricted mobility do not seem to mix with adsorbed IPA. In contrast, condensed water at $P_{water}/P_{0\text{-water}} > 0.5$ does have an effect on IPA T_1 as mixing between adsorbed water and adsorbed IPA takes place.

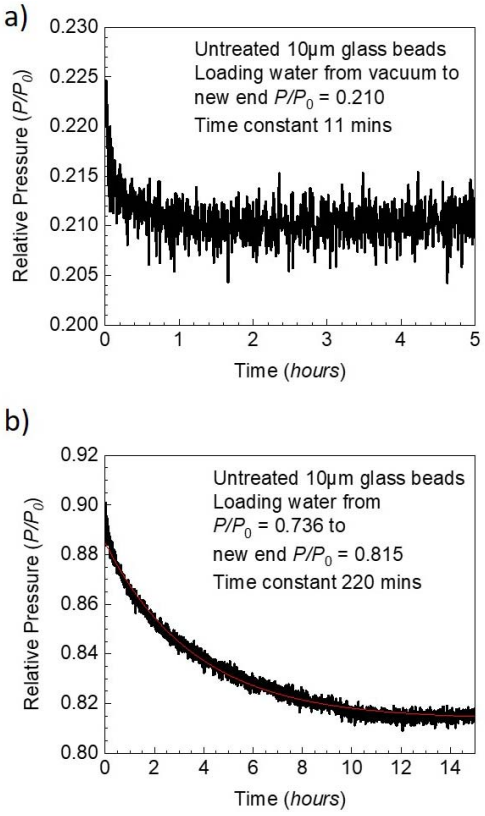

Fig. 3 (a) Pressure tracking of water loading from vacuum to $P/P_0 = 0.210$ on 10 µm untreated glass beads; (b) Pressure tracking of water loading from P/P_0=0.0.736 to 0.815 on 10 µm untreated glass beads

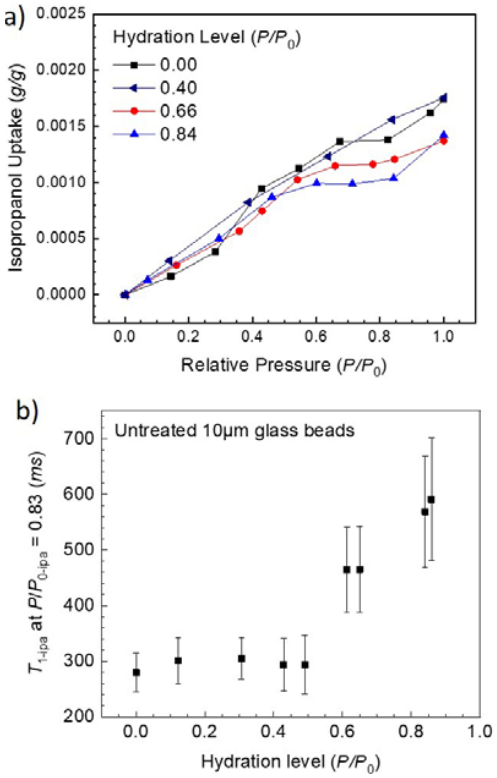

Fig. 4 (a) IPA adsorption on 10 µm untreated glass beads with different pre-adsorbed levels of hydration; (b) The -CH_3 ^{1}H spin-lattice relaxation time of IPA at IPA partial relative pressure of 0.83

We next investigate the adsorption on hydrophilic treated glass beads. Fig. 5 shows the results of the competitive adsorption of water and IPA on hydrophilic glass beads. Here, we first exposed $P_{water}/P_{0\text{-water}} = 0.07$ of water to the system. Even at this low relative pressure, as the surface is hydrophilic, the amount of water adsorption is 0.033 g/g, corresponding to 170 water layers on hydrophilic glass bead surface. We then introduce $P_{IPA}/P_{0\text{-IPA}} = 0.123$ IPA to the system and immediately after this, we followed the time dependences of the water proton peak and the IPA -CH_3 proton peak. Figs. 5 (a) and (b) show the water proton peak intensity and IPA-CH_3 proton peak intensity versus time after the $P_{IPA}/P_{0\text{-IPA}} = 0.123$ IPA exposure. Some of the corresponding ^{1}H NMR spectra are shown in Fig. 5 (c). The linewidth of water on hydrophilic treated sample is broader than the untreated one. The peak of methyl group also overlaps with the tail of the water peak. The methyl peak reaches equilibrium in less than 30 mins. It is very interesting to note that the water peak decreases in intensity after IPA exposure as shown in Fig. 5 (b). Fig. 5 (c) shows several examples of the ^{1}H NMR spectra to illustrate these changes mentioned. Here, the first spectrum after IPA exposure at waiting time 3.2 mins shows an increase of the water peak. This increase is an "artefact" due to the IPA vapor loading procedure. When we add IPA, the vapor system already has water vapor at pressure $P_{water}/P_{0\text{-water}} = 0.07$. By adding IPA to increase the total pressure, the initial water vapor is pushed toward the glass beads sample region giving rise to a temporary

increase of local water vapor pressure at the sample, leading to a temporary increase of water adsorption. As water and IPA vapors mix after a certain time, the partial pressure in the system becomes homogeneous and the water peak then decreases. However, the water peak intensity decreases far below the initial peak intensity before the IPA exposure. IPA makes the adsorbed water (hundreds of layers) unstable. Dissolving IPA in such water on hydrophilic surface makes the water unstable and this is very interesting. This reveals that such water on hydrophilic surface is different from bulk water. The destabilization of surface water by IPA is also reflected by the system pressure changes. Fig. 5 (d) shows the pressure of the system after IPA loading. The inset shows the pressure change in the first 5 minutes. During this time period, the adsorption rate (adsorption of water and IPA) of the system is higher than the desorption rate. Hence, the total number of vapor molecules in the glass system decreases, resulting in the initial decreases of the total pressure. After this time period, the pressure starts to increase. In this stage, the desorption rate is dominated by water desorption as measured by in-situ NMR shown in Fig. 5 (b).

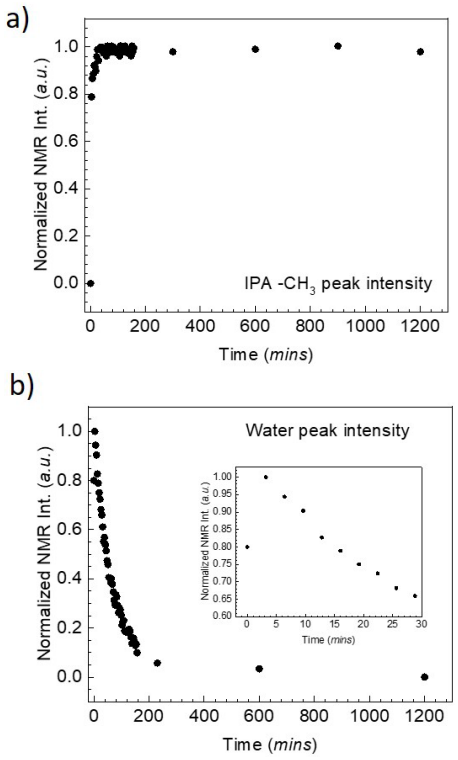

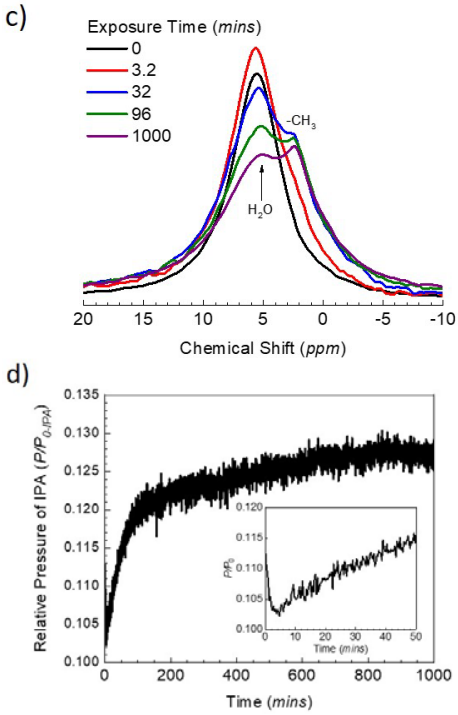

Fig. 5 (a) The IPA methyl ^{1}H NMR peak intensity versus time after IPA exposure of 10 µm hydrophilic treated glass beads with pre-adsorbed water; (b) The water ^{1}H NMR peak intensity versus time after IPA exposure; (c) The ^{1}H NMR spectra at different times after IPA exposure; (d) The pressure tracking of competitive adsorption on 10 µm hydrophilic glass beads.

Finally, we investigated the adsorption isotherm on hydrophobic surface. Fig. 6 compares the water uptake before takeoff over surface area for untreated glass beads and hydrophobic treated glass beads. We observe that after the sample is treated by chloro(dodecyl)dimethylsilane, the water uptake per surface area is much smaller and there is no uptake above $P/P_0 = 0.6$ as observed in the untreated sample shown in Fig. 2 (a). Only a few layers of water could adsorb on the surface of such hydrophobic treated glass beads.

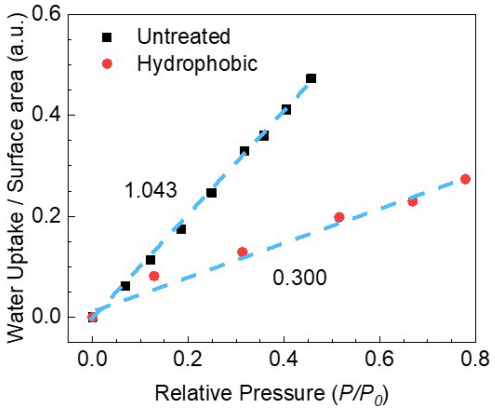

Fig. 6 Wettability of untreated glass beads (black square) and hydrophobic treated glass beads (red dot)

IV. Conclusion

In this study, we investigated water and IPA adsorption isotherms on glass beads with different hydrophilicity. In-situ NMR gas isotherm technique is used to conduct these measurements. Furthermore, the behavior of competitive adsorption is also investigated by studying IPA adsorption on glass beads with pre-adsorbed water. We investigated the same glasses beads treated with three different hydrophilicities. It is shown that water adsorption takes place in all three different samples, a couple of layers on the glass bead surface with hydrophobic treatment, about 6 layers on the surface with intermediate hydrophilicity, and over hundred layers on the hydrophilic surface. It is shown that water molecules of the 6 surface adsorbed layers on the untreated glass beads have restricted mobility as reflected by spin-lattice and spin-spin relaxation measurements. Competitive adsorption between IPA and water shows that such surface adsorbed water with restricted mobility does not mix with surface adsorbed IPA (mesoscopic phase separation). There is unusually large amount of adsorbed water (over 100 layers) at very low water vapor pressure on hydrophilic treated glass beads. Competitive adsorption shows that IPA adsorption makes such adsorbed water unstable. Further systematic studies of such abnormal surface water are currently underway. Such understanding of surface water on molecular level could enable us to arrive at a practical procedure to characterize wettability based on NMR measurements.

Acknowledgment

This work is supported by funding from the Saudi Aramco.

References

[1] Forrest F. Craig, J., *The Reservoir Engineering Aspects of Waterflooding.* Society of Petroleum Engineers of AIME, New York, 1971.

[2] Amott, E., *Observations Relating to the Wettability of Porous Rock*. 1959, Society of Petroleum Engineers. p. 7.

[3] Donaldson, E.C., et al., *Equipment and procedures for fluid flow and wettability tests of geological materials*. 1980: United States.

[4] Brown, R.J.S. and I. Fatt, *Measurements Of Fractional Wettability Of Oil Fields' Rocks By The Nuclear Magnetic Relaxation Method*, in *Fall Meeting of the Petroleum Branch of AIME*. 1956, Society of Petroleum Engineers: Los Angeles, California. p. 4.

[5] Devereux, O.F., *Effect of Crude Oil on the Nuclear Magnetic Relaxation of Water Protons in Sandstone.* Nature, 1967. 215(5101): p. 614-615.

[6] Hsu, W.-F., X. Li, and R.W. Flumerfelt, *Wettability of Porous Media by NMR Relaxation Methods*, in *SPE Annual Technical Conference and Exhibition*. 1992, Society of Petroleum Engineers: Washington, D.C. p. 11.

[7] Daughney, C.J., T.R. Bryar, and R.J. Knight, *Detecting Sorbed Hydrocarbons in a Porous Medium Using Proton Nuclear Magnetic Resonance.* Environmental Science & Technology, 2000. 34(2): p. 332-337.

[8] Looyestijn, W.J. and J. Hofman, *Wettability-Index Determination by Nuclear Magnetic Resonance.* SPE Reservoir Evaluation & Engineering, 2006. 9(02): p. 146-153.

[9] Song, Y., et al., *Hydrophilic and Hydrophobic Characteristics of Reservoir Rocks Quantified by Nuclear Magnetic Resonance-Detected Water Isotherms.* The Journal of Physical Chemistry C, 2019. 123(10): p. 6107-6113.

[10] Zhao, L., et al., *Reversible State Transition in Nanoconfined Aqueous Solutions.* Physical Review Letters, 2014. 112(7): p. 078301.